

# Wormlike Micelles with Microphase-Separated Cores from Blends of Amphiphilic AB and Hydrophobic BC Diblock Copolymers

Jintao Zhu and Ryan C. Hayward\*

Department of Polymer Science and Engineering, University of Massachusetts, Amherst, Massachusetts 01003

Received August 5, 2008

Revised Manuscript Received September 19, 2008

**Introduction.** Multicompartment block copolymer micelles composed of a water-soluble corona and a microphase-separated hydrophobic core have received attention for their potential applications in drug delivery, nanotechnology, and catalysis.<sup>1–3</sup> The presence of distinct chemical environments within the micellar core presents the opportunity to selectively entrap and release multiple different hydrophobic ingredients, with a corresponding enhancement in functionality over simple micellar structures containing only a single hydrophobic environment.<sup>4</sup> Recent work on multicompartment micelles has generally employed linear or starlike ABC triblock copolymers,<sup>2,4–15</sup> or multiblock copolymers such as ABCA<sup>16,17</sup> and ABCBA,<sup>18</sup> where A represents the hydrophilic block and B and C represent different hydrophobic blocks. The ability to tailor the overall size and shape of the aggregates as well as the internal arrangement of hydrophobic components is key to controlling the properties of multicompartment micelles. Through proper choice of the architecture and composition of the block copolymer and processing conditions, it has been possible to achieve a wide diversity of multicompartment micelle structures, including core–shell–corona spheres,<sup>5,8</sup> cylinders<sup>6,18</sup> and helices,<sup>13</sup> segmented wormlike micelles,<sup>2,9,10,12,15</sup> disks,<sup>7</sup> plates,<sup>17</sup> toroids,<sup>11</sup> and “raspberry-like” micelles.<sup>14</sup>

Another approach to tune the morphology of polymer micelles is to blend two or more different block copolymers. While the possibility of macrophase separation can limit the efficacy of this technique, the ability to mix the polymers in varying ratios presents a simple way to systematically tune micelle structure without having to synthesize a range of multiblock copolymers of varying composition. It is well-established that binary blends of AB diblock copolymers with the same chemical structure, but different molecular weights and block ratios, provide an effective way to control micellar size and structure.<sup>19–23</sup> Similarly, a number of strategies have been developed to prepare micelles with multicompartment hydrophobic cores using blends. For example, Webber and co-workers have created spherical core–shell–corona micelles using blends of AB and BC diblock copolymers by taking advantage of a B block with pH-dependent water solubility.<sup>24</sup> Lodge and co-workers have used blends of AB diblocks with starlike ABC triblocks,<sup>25</sup> and Pochan and co-workers have used blends of ABC and ABD triblock copolymers<sup>12</sup> to tune morphologies of multicompartment micelles.

In this report, we introduce a simple route to prepare wormlike micelles with microphase-separated cores by blending an amphiphilic AB diblock copolymer with several different hydrophobic BC diblock copolymers. Micelles are prepared using an emulsion route,<sup>23,26</sup> wherein an organic phase of polystyrene-*b*-poly(ethylene oxide) (PS<sub>9.5K</sub>–PEO<sub>5K</sub>) dissolved

in chloroform is dispersed as droplets in water. As we recently reported,<sup>23</sup> evaporation of solvent from these emulsion droplets gives rise to a hydrodynamic instability of the organic/water interface, leading to dispersal of the copolymer as wormlike micelles in the aqueous phase. Here, we investigate how the addition of hydrophobic BC diblock copolymers, such as PS-*b*-poly(vinylpyridine) or PS-*b*-polyisoprene, influences the morphology of the resulting micelles. We find that, under appropriate conditions, the hydrophobic block copolymer is successfully encapsulated into the cores of wormlike micelles. Microphase separation of the BC copolymer leads to multicompartment core–shell–corona micelles with structures that can be tuned from spherical to cylindrical core domains of the C block by varying the relative amounts of AB and BC copolymers.

**Experimental Section.** Preparation of multicompartment micelles was conducted by first dissolving PS<sub>9.5K</sub>–PEO<sub>5K</sub> in chloroform along with one of nine different hydrophobic diblock copolymers consisting of a polystyrene block and one of the following: poly(2-vinylpyridine) (P2VP), poly(4-vinylpyridine) (P4VP), poly(1,4-isoprene) (PI), or poly(1,4-butadiene) (PB) (see Table 1 for a complete list). The total polymer concentration was kept fixed at 10 mg/mL, while the ratio of the two polymers was varied between 0 and 100 wt % of the hydrophobic copolymer. This solution was then emulsified, via vigorous shaking by hand, into a continuous phase of deionized water containing 5 mg/mL of poly(vinyl alcohol) (*M*<sub>w</sub> = 13–23 kg/mol, 87–89% hydrolyzed) to stabilize droplets against coalescence. Emulsions were initially prepared with a volumetric ratio of organic to aqueous phases of 1:5; following emulsification, they were further diluted by a factor of 3–10 into deionized water. Emulsion droplets (initial diameters of ~5–100 μm) were allowed to settle to the bottom of an open glass container, and chloroform was evaporated into the surrounding air, with gentle magnetic stirring to increase the rate of solvent evaporation. All diblock copolymers were obtained from Polymer Source, while other chemicals were obtained from Aldrich.

Observation of the shrinking emulsion droplets containing copolymer blends was conducted using a Zeiss Axiovert 200 optical microscope. The resulting aggregate morphologies were observed via transmission electron microscopy (TEM) by drying a drop of aqueous micellar solution on a TEM grid coated with a carbon film and performing bright-field imaging using a JEOL 2000FX microscope operated at 200 kV. To resolve the microphase-separated structures within micelle cores, samples

**Table 1. Characteristics of the Hydrophobic BC Diblock Copolymers Employed**

copolymer	<i>M</i> <sub>n</sub> (kg/mol)	<i>w</i> <sub>PS</sub>	maximum content (wt %)
			dispersed uniformly in wormlike micelles <sup>a</sup>
PS <sub>56K</sub> –P2VP <sub>21K</sub>	77	0.73	40
PS <sub>55K</sub> –P2VP <sub>50K</sub>	105	0.52	—
PS <sub>19K</sub> –P4VP <sub>5.2K</sub>	24.2	0.79	30
PS <sub>12K</sub> –P4VP <sub>11.8K</sub>	23.8	0.50	—
PS <sub>36K</sub> –PI <sub>17K</sub>	53	0.68	40
PS <sub>25.8K</sub> –PI <sub>20.1K</sub>	45.9	0.56	—
PS <sub>16.5K</sub> –PI <sub>30.5K</sub>	47	0.35	—
PS <sub>35K</sub> –PB <sub>11K</sub>	46	0.76	—
PS <sub>9.4K</sub> –PB <sub>9K</sub>	18.4	0.51	—

<sup>a</sup> Samples are marked as showing negligible dispersibility when macrophase separation was observed at the lowest content of BC copolymer examined (10 wt %).

\* Corresponding author. E-mail: rhayward@mail.pse.umass.edu.

were stained by adding 0.05 wt % of  $\text{OsO}_4$  to the solution after removal of chloroform and prior to dispersal on a TEM grid (for blends containing PS-PI or PS-PB) or by exposing dried aggregates to  $\text{I}_2$  vapor for 2 h immediately before TEM observation (for blends with PS-P2VP or PS-P4VP).

**Results and Discussion.** We first considered blends of  $\text{PS}_{9.5\text{K}}\text{-PEO}_{5\text{K}}$  with the hydrophobic diblock copolymer  $\text{PS}_{56\text{K}}\text{-P2VP}_{21\text{K}}$ . When chloroform was evaporated from emulsion droplets containing solely the amphiphilic copolymer  $\text{PS}_{9.5\text{K}}\text{-PEO}_{5\text{K}}$ , the organic/water interface underwent a hydrodynamic instability in which droplets spontaneously ejected wormlike micelles into the aqueous phase, as reported previously.<sup>23</sup> In contrast, when only the hydrophobic copolymer  $\text{PS}_{56\text{K}}\text{-P2VP}_{21\text{K}}$  was present in the droplets, no interfacial instability was observed, and the end result was micrometer-sized spherical particles within which the polymer was microphase separated into cylindrical microdomains of P2VP. (We note that when the pH of the aqueous phase was lowered below  $\sim 4.5$ , PS-P2VP behaved as an amphiphile and gave rise to the same sorts of instabilities seen with PS-PEO.)

We next studied the evolution of  $\text{PS}_{9.5\text{K}}\text{-PEO}_{5\text{K}}$  wormlike micelle structures as increasing amounts of  $\text{PS}_{56\text{K}}\text{-P2VP}_{21\text{K}}$  were added to the emulsified polymer solution. When the blends contained modest amounts of PS-P2VP (20–40 wt % of the total polymer concentration), droplets continued to undergo interfacial instabilities upon solvent removal, generating wormlike micelles (see movie 1 of the Supporting Information for a real-time video of the process of micelle formation at a composition of 20 wt % PS-P2VP). TEM imaging of the resulting samples, after exposure to  $\text{I}_2$  vapor to stain the P2VP domains, revealed that  $\text{PS}_{56\text{K}}\text{-P2VP}_{21\text{K}}$  was uniformly incorporated into the micelle cores, as shown in Figure 1. When the content of the hydrophobic polymer was 20 wt % (Figure 1a), the micelle cores showed microphase separation into spherical P2VP domains within a PS shell. The sizes of P2VP spheres was fairly uniform (mean diameter 15 nm, standard deviation 2 nm), and the overall diameter of the wormlike micelles was  $41 \pm 4$  nm, as compared to  $29 \pm 1$  nm for neat PS-PEO micelles. At 30 wt %  $\text{PS}_{56\text{K}}\text{-P2VP}_{21\text{K}}$  (Figure 1b), a bimodal distribution of P2VP sphere sizes was observed, with smaller spheres nearly the same size as those at 20 wt % (diameters  $13 \pm 3$  nm), while the larger spheres were  $29 \pm 4$  nm. Wherever large spheres were observed, the overall diameter of the wormlike micelle was locally expanded, leading to an undulation in the micelle size. A few of the larger aggregates were actually prolate ellipsoids, with a slight elongation along the direction of the cylinder axis. When the content of  $\text{PS}_{56\text{K}}\text{-P2VP}_{21\text{K}}$  was further increased to 40 wt %, the hybrid micelles consisted of coaxial cylindrical structures with P2VP cores, PS shells, and PEO coronae (Figure 1c). The diameter of the P2VP cores were  $16 \pm 2$  nm, while the overall wormlike micelle diameters were  $60 \pm 6$  nm, roughly double that of neat  $\text{PS}_{9.5\text{K}}\text{-PEO}_{5\text{K}}$  micelles. The narrow distribution of micelle sizes indicates that the distribution of PS-P2VP within the composite micelles was highly uniform. A small fraction of the material ( $\sim 5$  vol %) formed concentric spherical core-shell-corona structures, as indicated by the arrow in Figure 1c.

An increase in  $\text{PS}_{56\text{K}}\text{-P2VP}_{21\text{K}}$  content to 50 wt % led to formation of thicker “lumps” of excess PS-P2VP along the cylindrical micelles, as shown in Figure 2a. Careful examination of this and other TEM images revealed that the PS-P2VP copolymer inside these lumps was microphase separated primarily into cylindrical domains of P2VP with diameters of  $17 \pm 3$  nm. In nearly all cases, the cylinder axes were oriented

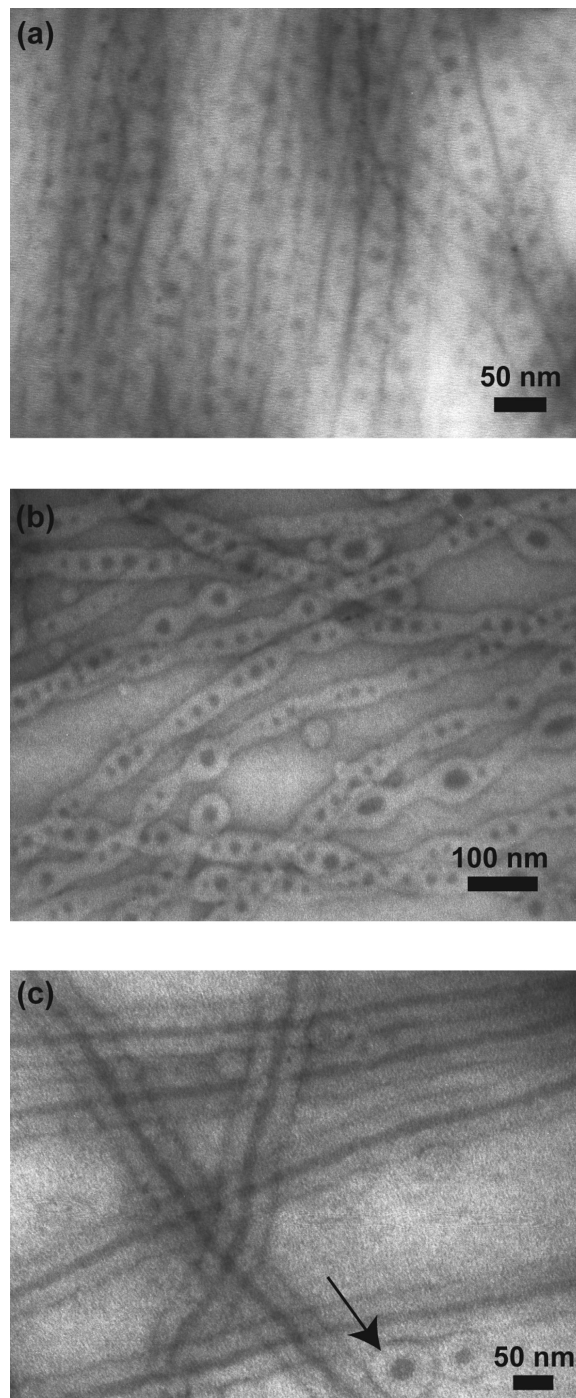


**Figure 1.** Bright field TEM images showing the evolution of structures of multicompart ment wormlike micelles formed from blends of  $\text{PS}_{9.5\text{K}}\text{-PEO}_{5\text{K}}$  with  $\text{PS}_{56\text{K}}\text{-P2VP}_{21\text{K}}$  in weight ratios of (a) 80:20, (b) 70:30, and (c) 60:40. P2VP regions were stained dark by exposure to  $\text{I}_2$  vapor. The wormlike micelles showed internal microphase separation into (a, b) spherical and (c) cylindrical P2VP cores surrounded by PS shells.

perpendicular to the long direction of the wormlike micelle, forming rings or coils that give rise to the dark circular features in Figure 2. Similar toroidal and coiled morphologies have been experimentally observed and theoretically predicted for cylinder-forming block copolymers under rigid cylindrical confinement.<sup>27–33</sup> Regions of the wormlike micelles in-between the lumps showed predominantly a coaxial cylindrical structure similar to that observed at 40 wt % PS-P2VP (Figure 1c). Apparently, the cylindrical micelles became “saturated” with hydrophobic diblock copolymer at around 40 wt %, and addition



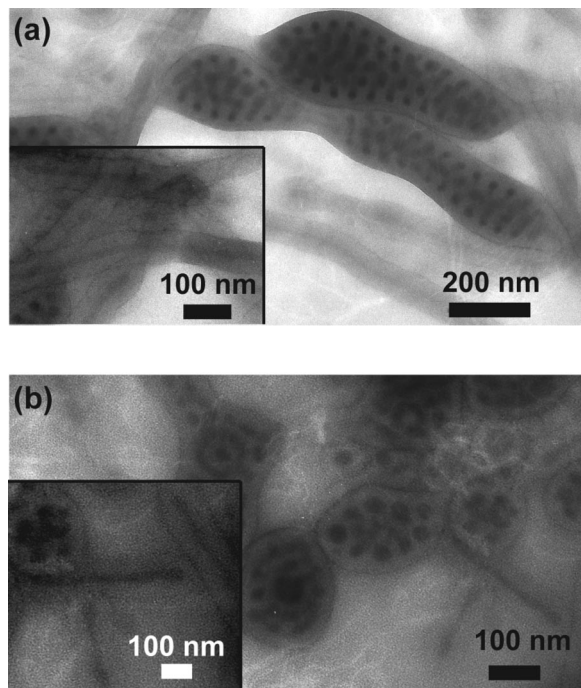


**Figure 2.** Bright field TEM images of the microstructures formed by blends of PS<sub>9.5K</sub>–PEO<sub>5K</sub> with PS<sub>56K</sub>–P2VP<sub>21K</sub> in weight ratios of (a) 50:50 and (b) 20:80. P2VP regions were stained dark by exposure to I<sub>2</sub> vapor. Excess PS–P2VP was observed to macrophase separate into (a) lumps along wormlike micelles and (b) discrete particles, with the remainder of the material forming wormlike micelles with primarily cylindrical P2VP cores (insets are contrast adjusted to more clearly reveal the core–shell–corona cylindrical micelles).

of more PS–P2VP led to macrophase separation into domains that could adopt nearly the equilibrium bulk structure of the block copolymer. Observation by optical microscopy (see movie 2 of the Supporting Information) showed a qualitatively different mechanism of formation, with a large number of micelles simultaneously growing radially outward from each droplet, as opposed to the “spinning” of individual fluid fibers and stepwise fragmentation of drops observed at 20 wt % PS–P2VP. However, no clear indication was detected of the stage at which macrophase separation occurred, presumably due to the small sizes of phase-separated lumps. The time scale over which the instability occurred was not very sensitive to the composition of the blend: from the point where initial roughening of a droplet’s surface was observed until no further structural changes could be detected was  $\sim 2$  min in all cases.

A further increase of PS<sub>56K</sub>–P2VP<sub>21K</sub> content to 80 wt % led an initial roughening of the droplet surface and ejection of micelles, but after a few seconds the instability came to a halt, with most of the material within the droplet remaining as a large microparticle (see movie 3 of the Supporting Information). As shown in Figure 2b, even the material dispersed through the instability showed considerable macrophase separation, with polydisperse particles of PS–P2VP ( $\sim 100$  nm– $2$   $\mu$ m diameters) coexisting with wormlike micelles internally microphase separated into cylinders or in some cases spheres of P2VP. At 90 wt % PS–P2VP, interfacial instabilities were largely suppressed, and the resulting morphology was polydisperse microparticles with internal organization into spheres and cylinders of P2VP. Presumably, PS–PEO must form a thin layer coating the surfaces of these microparticles.

Together, the data in Figures 1 and 2 demonstrate that PS<sub>56K</sub>–P2VP<sub>21K</sub> is uniformly incorporated into cylindrical micelles of PS<sub>9.5K</sub>–PEO<sub>5K</sub> up to a miscibility limit of roughly

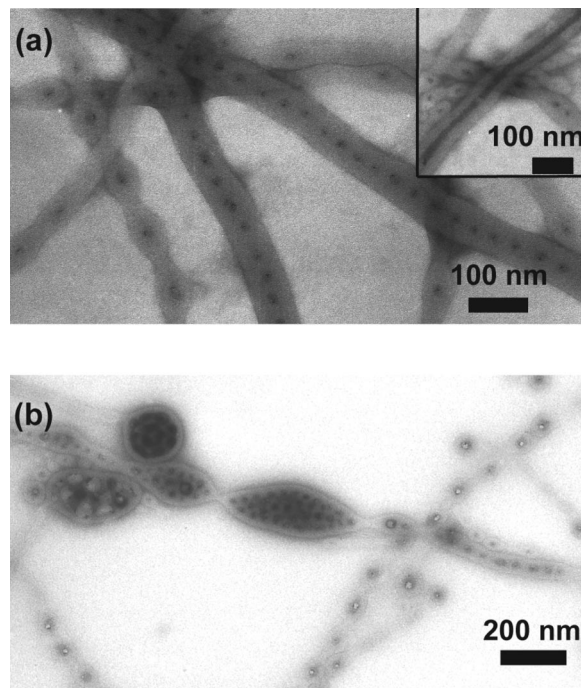


**Figure 3.** Bright field TEM images of multicompartment wormlike micelles formed by blending PS<sub>9.5K</sub>–PEO<sub>5K</sub> with PS<sub>36K</sub>–PI<sub>17K</sub> in weight ratios of (a) 80:20 and (b) 40:60. PI domains were stained dark with OsO<sub>4</sub>. (a) At 20 wt % PS–PI, wormlike micelles showed internal microphase separation into spherical (and occasionally cylindrical; inset) domains of PI. (b) At 60 wt % PS–PI, macrophase separation into lumps and particles of PS–PI was observed.

40 wt %, beyond which point the micelles become saturated and begin to exclude PS–PVP as a separate phase. Since the structural organization of the polymer takes place fairly rapidly (presumably on a time scale of seconds) as chloroform is removed, it is not clear that this behavior represents thermodynamic equilibrium, but the uniformity of structures observed and the appearance of macrophase separation beyond a well-defined composition suggest that the hybrid micelles are at least able to approach structures corresponding to local energy minima. The evolution of the internal structures of multicompartment micelles from small spheres to mixtures of large and small spheres and finally to cylinders with increasing content of PS–P2VP is similar to the predictions of Shi and co-workers for cylinder-forming block copolymers confined to very small rigid cylinders;<sup>31,33</sup> however, the soft nature of the confinement here provides an additional degree of freedom.

To determine the role played by hydrophobic block copolymer composition on the formation of multicompartment micelles, we studied a series of eight other BC diblock copolymers (Table 1), where the B block was always PS, but the C block consisted of P2VP, PI, P4VP, or PB. For two other diblock copolymers, PS<sub>19K</sub>–P4VP<sub>5.2K</sub> and PS<sub>36K</sub>–PI<sub>17K</sub>, with weight fractions of PS ( $w_{PS}$ ) of 0.79 and 0.68, respectively, similar behaviors to that of PS<sub>56K</sub>–P2VP<sub>21K</sub> ( $w_{PS} = 0.73$ ) were observed, as shown for PS<sub>36K</sub>–PI<sub>17K</sub> in Figure 3. At low content of the BC diblock copolymers, both were uniformly incorporated into cylindrical micelles with organization of the C block predominantly into spherical domains. Beyond certain miscibility limits (30 wt % for PS<sub>19K</sub>–P4VP<sub>5.2K</sub> and 40 wt % for PS<sub>36K</sub>–PI<sub>17K</sub>), macrophase separation occurred. Surprisingly, another copolymer of similar composition, PS<sub>35K</sub>–PB<sub>11K</sub> ( $w_{PS} = 0.76$ ), could only be incorporated into wormlike micelles in sparing amounts, with

macrophase separation into lumps of hydrophobic diblock copolymer occurring even at 10 wt %.

Each of the other five copolymers studied, with  $w_{PS}$  varying between 0.35 and 0.56 as summarized in Table 1, also showed negligible incorporation into wormlike micelles. In each case, addition of 10 wt % of the hydrophobic diblock led to macrophase separation into domains of the BC copolymer and few if any microdomains of the C block within PS-PEO wormlike micelles. It is not surprising that these polymers are not incorporated into wormlike micelles in appreciable amounts, since their equilibrium structures are lamellae (or cylinders of PS in a matrix of PI for PS<sub>16.5K</sub>-PI<sub>30.5K</sub>), and therefore they must pay significant energy penalties to confine the C block to spherical or cylindrical microdomains within the micelle core. However, these observations further suggest that multicomponent micelles are able to equilibrate their structures to some degree, rather than simply representing kinetically trapped states. Generalizing from these results, it appears that BC diblock copolymers containing 70–80 wt % PS as the B block can typically be incorporated into the cores of wormlike micelles of PS<sub>9.5K</sub>-PEO<sub>5K</sub> up to reasonably high concentrations (30–40 wt %), while polymers with lower contents of PS are not incorporated in significant amounts. The relative molecular weights of the PS blocks of the two copolymers are also likely to play an important role in this process; however, the polymers investigated to date do not allow any systematic comparisons regarding molecular weight to be made.

In summary, we have introduced a simple way to prepare multicompartment wormlike micelles via interfacial instabilities of chloroform-in-water emulsion droplets containing binary blends of amphiphilic AB and hydrophobic BC diblock copolymers. For appropriate compositions, the BC copolymer was uniformly incorporated into the cores of wormlike micelles, where it microphase separated into spherical or cylindrical microdomains of the C block, depending on the content of BC copolymer in the blend. The composition of the BC copolymer plays an important role in this process, with asymmetric polymers containing longer B blocks generally allowing successful formation of multicompartment wormlike micelles.

**Acknowledgment.** We gratefully acknowledge funding for this work provided by the National Science Foundation through Grant CBET 0741885 and the MRSEC at UMass (DMR 0213695).

**Supporting Information Available:** Real-time movies showing the evolution of droplet structures at PS<sub>56K</sub>-P2VP<sub>21K</sub> concentrations of 20 wt % (movie 1), 50 wt % (movie 2), and 80 wt % (movie 3). This material is available free of charge via the Internet at <http://pubs.acs.org>.

## References and Notes

- (1) Laschewsky, A. *Curr. Opin. Colloid Interface Sci.* **2003**, *8* (3), 274–281.
- (2) Li, Z. B.; Kesselman, E.; Talmon, Y.; Hillmyer, M. A.; Lodge, T. P. *Science* **2004**, *306* (5693), 98–101.
- (3) Lutz, J. F.; Laschewsky, A. *Macromol. Chem. Phys.* **2005**, *206* (8), 813–817.
- (4) Lodge, T. P.; Rasdal, A.; Li, Z. B.; Hillmyer, M. A. *J. Am. Chem. Soc.* **2005**, *127* (50), 17608–17609.
- (5) Gohy, J. F.; Willet, N.; Varshney, S.; Zhang, J. X.; Jérôme, R. *Angew. Chem., Int. Ed.* **2001**, *40* (17), 3214–3216.
- (6) Lei, L. C.; Gohy, J. F.; Willet, N.; Zhang, J. X.; Varshney, S.; Jérôme, R. *Macromolecules* **2004**, *37* (3), 1089–1094.
- (7) Zhou, Z. L.; Li, Z. B.; Ren, Y.; Hillmyer, M. A.; Lodge, T. P. *J. Am. Chem. Soc.* **2003**, *125* (34), 10182–10183.
- (8) Lodge, T. P.; Hillmyer, M. A.; Zhou, Z. L.; Talmon, Y. *Macromolecules* **2004**, *37* (18), 6680–6682.
- (9) Li, Z. B.; Hillmyer, M. A.; Lodge, T. P. *Nano Lett.* **2006**, *6* (6), 1245–1249.
- (10) Li, Z. B.; Hillmyer, M. A.; Lodge, T. P. *Langmuir* **2006**, *22* (22), 9409–9417.
- (11) Pochan, D. J.; Chen, Z. Y.; Cui, H. G.; Hales, K.; Qi, K.; Wooley, K. L. *Science* **2004**, *306* (5693), 94–97.
- (12) Cui, H. G.; Chen, Z. Y.; Zhong, S.; Wooley, K. L.; Pochan, D. J. *Science* **2007**, *317* (5838), 647–650.
- (13) Zhong, S.; Cui, H. G.; Chen, Z. Y.; Wooley, K. L.; Pochan, D. J. *Soft Matter* **2008**, *4* (1), 90–93.
- (14) Kubowicz, S.; Baussard, J. F.; Lutz, J. F.; Thünemann, A. F.; von Berlepsch, H.; Laschewsky, A. *Angew. Chem., Int. Ed.* **2005**, *44* (33), 5262–5265.
- (15) Zhu, J. T.; Jiang, W. *Macromolecules* **2005**, *38* (22), 9315–9323.
- (16) Brannan, A. K.; Bates, F. S. *Macromolecules* **2004**, *37* (24), 8816–8819.
- (17) Gomez, E. D.; Rappl, T. J.; Agarwal, V.; Bose, A.; Schmutz, M.; Marques, C. M.; Balsara, N. P. *Macromolecules* **2005**, *38* (9), 3567–3570.
- (18) Thünemann, A. F.; Kubowicz, S.; von Berlepsch, H.; Möhwald, H. *Langmuir* **2006**, *22* (6), 2506–2510.
- (19) Terreau, O.; Bartels, C.; Eisenberg, A. *Langmuir* **2004**, *20* (3), 637–645.
- (20) Jain, S.; Bates, F. S. *Macromolecules* **2004**, *37* (4), 1511–1523.
- (21) Cai, P.; Wang, C. Q.; Ye, J.; Xie, Z. W.; Chi, W. *Macromolecules* **2004**, *37* (9), 3438–3443.
- (22) Yoo, S. I.; Sohn, B. H.; Zin, W. C.; Jung, J. C.; Park, C. *Macromolecules* **2007**, *40* (23), 8323–8328.
- (23) Zhu, J. T.; Hayward, R. C. *J. Am. Chem. Soc.* **2008**, *130* (23), 7496–7502.
- (24) Talingting, M. R.; Munk, P.; Webber, S. E.; Tuzar, Z. *Macromolecules* **1999**, *32* (5), 1593–1601.
- (25) Li, Z. B.; Hillmyer, M. A.; Lodge, T. P. *Macromolecules* **2006**, *39* (2), 765–771.
- (26) Geng, Y.; Discher, D. E. *J. Am. Chem. Soc.* **2005**, *127* (37), 12780–12781.
- (27) Wu, Y. Y.; Cheng, G. S.; Katsov, K.; Sides, S. W.; Wang, J. F.; Tang, J.; Fredrickson, G. H.; Moskovits, M.; Stucky, G. D. *Nat. Mater.* **2004**, *3* (11), 816–822.
- (28) Xiang, H. Q.; Shin, K.; Kim, T.; Moon, S. I.; McCarthy, T. J.; Russell, T. P. *Macromolecules* **2004**, *37* (15), 5660–5664.
- (29) Xiang, H. Q.; Shin, K.; Kim, T.; Moon, S.; McCarthy, T. J.; Russell, T. P. *J. Polym. Sci., Part B: Polym. Phys.* **2005**, *43* (23), 3377–3383.
- (30) Feng, J.; Ruckenstein, E. *Macromolecules* **2006**, *39* (14), 4899–4906.
- (31) Yu, B.; Sun, P. C.; Chen, T. C.; Jin, Q. H.; Ding, D. T.; Li, B. H.; Shi, A. C. *Phys. Rev. Lett.* **2006**, *96* (13), 138306.
- (32) Li, W. H.; Wickham, R. A. *Macromolecules* **2006**, *39* (24), 8492–8498.
- (33) Chen, P.; Liang, H. J.; Shi, A. C. *Macromolecules* **2007**, *40* (20), 7329–7335.

MA801783M